Japanese Journal of Applied Physics **55**, 07KF13 (2016)
http://doi.org/10.7567/JJAP.55.07KF13

REGULAR PAPER

Three-dimensional visualization of shear wave propagation generated by dual acoustic radiation pressure

Yuta Mochizuki[1], Hirofumi Taki[1,2], and Hiroshi Kanai[2,1*]

[1]*Graduate School of Biomedical Engineering, Tohoku University, Sendai 980-8579, Japan*
[2]*Graduate School of Engineering, Tohoku University, Sendai 980-8579, Japan*

*E-mail: kanai@ecei.tohoku.ac.jp

Received November 14, 2015; revised March 2, 2016; accepted March 27, 2016; published online June 16, 2016

An elastic property of biological soft tissue is an important indicator of the tissue status. Therefore, quantitative and noninvasive methods for elasticity evaluation have been proposed. Our group previously proposed a method using acoustic radiation pressure irradiated from two directions for elastic property evaluation, in which by measuring the propagation velocity of the shear wave generated by the acoustic radiation pressure inside the object, the elastic properties of the object were successfully evaluated. In the present study, we visualized the propagation of the shear wave in a three-dimensional space by the synchronization of signals received at various probe positions. The proposed method succeeded in visualizing the shear wave propagation clearly in the three-dimensional space of 35 × 41 × 4 mm^3. These results show the high potential of the proposed method to estimate the elastic properties of the object in the three-dimensional space.

1. Introduction

It is well known that the progression of a lesion is accompanied by changes in the hardness of biological tissue. For example, owing to pyramidal tract disorders or peripheral neuropathy, the elastic modulus of muscle decreases. In amyloidosis, atrophy and the elevation of muscle hardness occur. Also, polymyositis and myoglobinuria lead to muscle weakness or a decrease in muscle elasticity.[1,2] Therefore, it would be valuable to measure the elasticity of muscle for the early detection and quantitative diagnosis of muscle disorder.

Ultrasound imaging is a noninvasive test with high performance in depicting soft tissue. Several methods have been reported for the improvement in image quality,[3–5] tissue characterization,[6–8] and the estimation of tissue displacement.[9–11] Many methods that can be used to noninvasively measure the hardness of soft biological tissue have been proposed; in these method, external pressure is applied to biological tissue and the resulting deformation and movement of the tissue are observed to obtain the parameters regarding the hardness of the tissue. Recently, some methods have been developed for the noninvasive evaluation of the elasticity of soft tissue.[12,13] Other research groups have reported several methods based on the hysteresis property between force and displacement,[14] and based on the dispersion of shear wave propagation velocity.[15]

Ultrasound-based measurement methods can be classified into two categories according to the methods used to apply pressure. One is the application of static pressure and the other is the application of dynamic pressure. In the former method, by measuring the deformation of the tissue with ultrasound before and after the application of static pressure, the elasticity of the biological tissue is estimated. However, the elasticity of the tissue cannot be evaluated quantitatively.[16] Therefore, our group has applied dynamic pressure produced by acoustic radiation to quantitatively evaluate the elastic properties of the tissue by the ultrasound measurement of the propagation of the generated shear wave.

Over the past decade, remote actuation methods based on acoustic radiation pressure have been reported. Fatemi and coworkers proposed an imaging modality that uses the acoustic response of an object, which is closely related to its mechanical properties. By measuring the acoustic emission with a hydrophone, hard inclusions, such as calcified tissues in soft materials, were detected experimentally.[17,18] However, the amplitude of the radiated acoustic emission signal was very small for soft tissue and the spatial resolution was limited by the size of the intersectional area of ultrasound beams at two slightly different frequencies.

Nightingale and coworkers proposed an alternative imaging method (acoustic radiation pressure impulse: ARFI), in which focused ultrasound is employed to apply radiation pressure to soft tissue for a short duration (less than 1 ms). The elastic properties of the tissue were investigated on the basis of the magnitude of the transient response, which was measured as the displacement of tissue with ultrasound.[19–21] However, in order to generate a measurable displacement by several successive ultrasound pulses, high-intensity pulsed ultrasound at 1,000 W/cm^2 was required. According to safety guidelines for the use of diagnostic ultrasound, it is recommended that the intensity be below 240 mW/cm^2 (ISPTA) for pulsed waves and 1 W/cm^2 for continuous waves.[22] The intensity of the pulsed ultrasound employed by Nightingale et al. was, therefore, far greater than that recommended in the safety guidelines.[19]

Subsequently, many groups studied methods for actuation using high-intensity pulsed ultrasound to measure elastic properties of biological tissue.[23,24] To decrease the ultrasound intensity for the actuation of soft tissue, our group chose continuous-wave ultrasound, as did Fatemi et al.,[17] in which the maximum intensity of 1 W/cm^2 for continuous waves given by safety guidelines generates an acoustic radiation pressure of 6.67 Pa, which is very small. Therefore, to generate a measurable displacement by acoustic actuation, an effective method of applying acoustic radiation pressure should be developed.

A single acoustic radiation pressure does not generate deformation effectively because it primarily changes the position of the object. Thus, our group has developed a method in which two cyclical radiation pressures are simultaneously applied to a phantom from two opposite horizontal directions to cyclically compress the object along the horizontal direction. Furthermore, the resultant regional displace-

ment and strain in the phantom simulating soft biological tissue or any type of tissue were measured using a different ultrasound probe. This method enables the effective generation of deformation by acoustic actuation.[25,26]

In another study using two sources of shear waves,[27] the mechanical properties of an object were evaluated by generating two shear waves that interfered with each other. However, this method requires that two shear wave sources be perfectly opposite, and that shear waves be insonified from the skin surface by an external vibrator.

Our group has proposed a method to actuate phantoms using dual acoustic radiation pressure and to measure the propagation velocity of the generated shear wave, from which the elastic properties of an object can be estimated.[28] However, the study reported the measurement of the shear wave propagation only in the vertical plane. In the present study, therefore, we propose a novel method that visualizes the propagation of the generated shear wave in a three-dimensional (3D) space in a medium. This method was applied to a phantom that simulates uniform soft tissue.

2. Experimental methods

2.1 Generation principle of the displacement inside the phantom due to acoustic radiation pressure

We apply an acoustic radiation pressure that consists of two continuous sinusoidal waves, whose center frequencies are f_0 and $(f_0 + \Delta f)$, to an object in a water tank. The acoustic pressure in the object is given by

$$p_{\mathrm{sum}}(d,t) = e^{-\alpha d}\{p_0 \cos(kd - 2\pi f_0 t) + p_0 \cos[kd - 2\pi(f_0 + \Delta f)t]\}, \quad (1)$$

where d, α, k, and p_0 are the distance from the object surface, the attenuation coefficient, the wave number, and the sound pressure in the object, respectively. The acoustic radiation pressure $P_{\mathrm{R}}(d,t)$ is given by

$$P_{\mathrm{R}}(d,t) \approx \frac{\alpha p_0^2}{\rho_2 c_2^2} e^{-2\alpha d}(1 + \cos 2\pi \Delta f t), \quad (2)$$

where ρ_2 and c_2 are the density and sound speed of the object, respectively. When the acoustic radiation pressure in Eq. (2) is generated in the phantom, a locally vibrated displacement is induced, and a shear wave propagates from the focal point.[28]

In the present study, we employed two focused transducers to generate a shear wave, where each transducer was applied by the overlaid component of the two continuous sinusoidal waves of f_0 and $(f_0 + \Delta f)$. To generate the shear wave effectively, both foci of the transducers were located at the same excitation position and both radiation directions were located in the same plane as shown in Fig. 1(a). The radiation direction of each transducer adopted an angle of 25° to the horizontal plane. Since the focal length of each transducer was 50 mm, the distance between the excitation position and each transducer surface was 91 mm.

As shown in Eq. (2), the acoustic radiation pressure $P_{\mathrm{R}}(d,t)$ vibrates from 0 to $(2\alpha p_0^2/\rho_2 c_2^2)\exp(-2\alpha d)$ at the frequency of Δf. Therefore, the region around the focal point vibrates in the depth direction at the frequency of Δf, and the shear wave propagates to the surrounding region as shown in Fig. 1(b). We measured the propagation of the shear wave by an ultrasound diagnostic equipment (Hitachi-Aloka Pro Sound F75) with a 7.5 MHz linear probe (Hitachi-Aloka UST-5415).

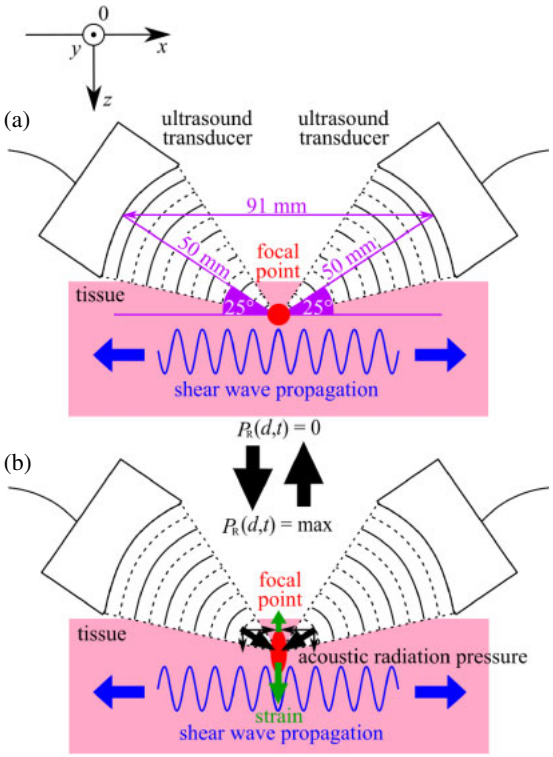

Fig. 1. (Color online) Schematic diagram showing the mechanism of the shear wave generation by irradiation dual acoustic pressure at the (a) minimum $[P_{\mathrm{R}}(d,t) = 0]$ and (b) maximum acoustic radiation pressures.

2.2 Measurement of the shear wave in 3D space

We prepared a phantom that consisted of 98% mass concentration silicone (Sin-Etsu Silicone KE114L) and 2% graphite powder. The dimensions of the phantom were 110, 150, and 34 mm in the x-, y-, and z-directions, respectively. Its density was 1,208 kg/m^3. The phantom was set in the water tank, whose dimensions were 450, 300, and 300 mm in the x-, y-, and z-directions, respectively.

For ultrasound measurement, the ultrasound diagnostic equipment with the linear probe of 7.5 MHz was employed. The frame rate was 521 Hz and the scan line interval was 3.3 mm. The number of beams used in the measurement was 11, and the beams were numbered from 0 to 10. As shown in Fig. 2, the foci of two focused transducers were set about 20 mm away from beam 0 for generating vibration with $\Delta f =$ 100 Hz. The acoustic radiation pressure was applied from the two focused transducers 1 min before the measurement.

The shear wave propagation was measured by shifting the ultrasound probe by 1 mm along the x-axis direction in the range from −20 to +20 mm. To detect the irradiation time of the acoustic radiation pressure at each measurement x-position, the input signal for the acoustic radiation pressure was input into the vital information acquisition port of the ultrasound diagnostic equipment, as shown in Fig. 2, where the sampling frequency of the acquisition system was 1 kHz. RF data at a measurement x-position along each of the 11 beams on the y–z plane had a synchronization signal. Consequently, all the signals received at various probe x-positions were synchronized.

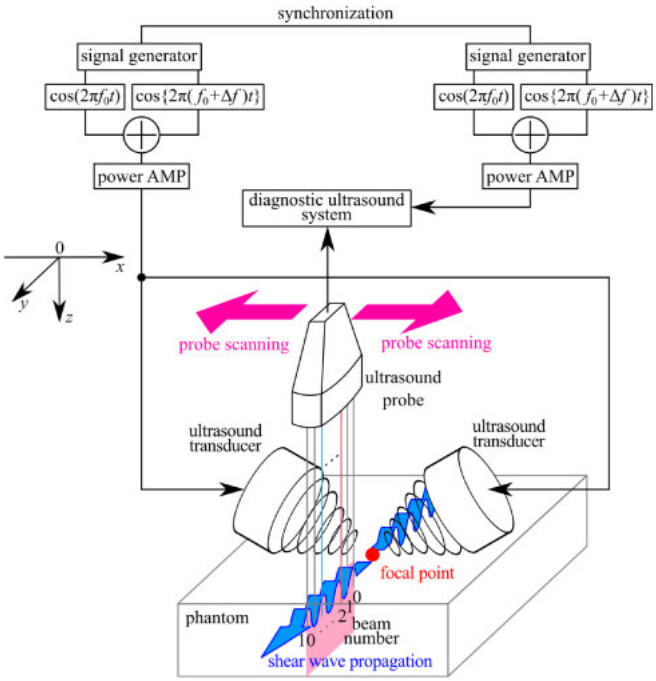

Fig. 2. (Color online) Measurement image for visualization in 3D space.

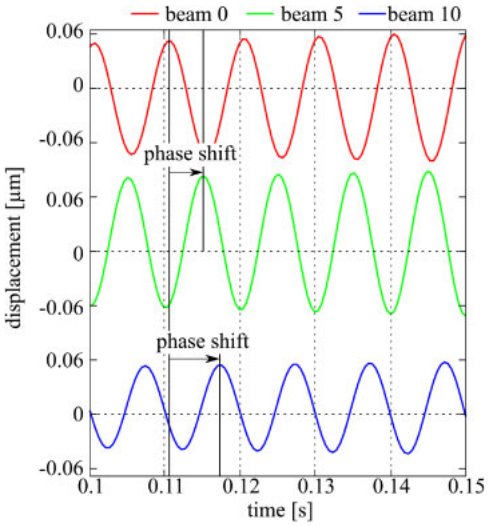

Fig. 3. (Color online) Displacements of the shear waves at the depth of $z = 1$ mm in the vertical direction in the plane of $x = -5$ mm.

In each y–z plane, there is a small delay of $174\,\mu s = 1/(11 \times 521)$ in acquisition time of RF data between the succeeding beams. However, it cannot be neglected to show the propagation of the shear wave generated by the acoustic radiation pressure ($\Delta f = 100$ Hz). Thus, in the present study, this delay time between the beams was deleted in the calculation process to show the phase of the shear wave component. Therefore, the propagation of the shear wave can be visualized in a 3D space.

The instantaneous velocity $v(t + \Delta t/2)$ was calculated from the phase shift from the received signal $b(t)$ to $b(t + \Delta t)$ after quadrature detection, where the phase shift was determined by an ultrasound correlation-based method, the *phased-tracking method*.[29,30] A FIR band-pass filter $H(f)$ was applied to the instantaneous velocity $v(t)$ to extract the frequency component of Δf. Then, the instantaneous velocity $v(t)$ was integrated to estimate the displacement waveform.

3. Results

Figure 3 shows the displacements of the shear waves at the depth of $z = 1$ mm in the vertical direction on the plane of $x = -5$ mm. In all of the three beams, the vibration frequency of the displacement was about 100 Hz, the difference frequency Δf. The phase shift of the displacement in beam 10 from the phase in beam 0 was larger than that in beam 5. Since beam 0 was located near the focal point as shown in Fig. 2, this result shows the propagation of the shear wave in the direction away from the focal point.

Figure 4 shows the amplitude and phase of the instantaneous velocity of the shear wave, $A_v(x, y, z, t)$ and $\theta_v(x, y, z, t)$, in four horizontal z-planes. Each horizontal z-plane was constructed by the synchronization of signals received at various probe positions using the input signal for the acoustic radiation pressure. As shown in Figs. 4(a) and 4(b), in the planes of $z = 0$ mm, $z = 3.0$ mm in depth, the shear wave clearly propagated in the direction away from the focal point. The cycle of the instantaneous velocity was about 10 ms, which corresponded to the difference frequency $\Delta f = 100$ Hz. This result shows the capability of the proposed method based on the synchronization process in the 3D visualization of the shear wave propagation.

Figure 5 shows the amplitude and phase of the instantaneous velocity of the shear wave, $A_v(x_0, y, z, t_0)$ and $\theta_v(x_0, y, z, t_0)$, in a vertical plane of $(x_0, t_0) = (-5\text{ mm}, 4\text{ ms})$. We succeeded in visualizing the propagation of the shear wave clearly in the direction away from the focal point within the depths from $z = 0$ to 4 mm.

Figure 6 shows the phase shift of the instantaneous velocity at a measurement point (x_0, y, z) from the phase at a reference point (x_0, y_0, z_0) given by

$$\theta_d(x_0, y, z) = E_t[\theta_v(x_0, y, z, t) - \theta_v(x_0, y_0, z_0, t)], \qquad (3)$$

where each value was averaged among 2,080 frames in $0 \le t \le 1$ s. We set the reference point at $(x_0, y_0, z_0) = (-5, 0, 0\text{ mm})$. We determined the propagation velocity of the shear wave using the least-mean-squares method. The velocity was estimated to be 4.5, 4.5, 4.7, and 4.7 m/s at the depths of $z = 0$, 1.0, 2.0, and 3.0 mm, respectively. In our previous study, it was reported that the propagation velocity of a 100 Hz shear wave was 3.5 m/s in a different phantom,[28] which is similar to the above result.

4. Discussion

The proposed method succeeded in visualizing the shear wave propagation clearly in the 3D space, as shown in Figs. 4 and 5, which show a high potential of the proposed method with a synchronization process. In the region of $x > 0$ in Figs. 4(a) and 4(b), the wavefront of the shear wave was not clearly visualized. On the other hand, at depths of $z = 6.0$ and 9.0 mm in Figs. 4(c) and 4(d), the shear wave propagation was difficult to observe. This asymmetry in the x-direction might be caused by the misalignment between the foci of the ultrasound transducers for actuation in the setting of the experiment.

The phase shift $\theta_d(x_0, y = 0, z = 3.0\text{ mm})$ at the leftmost side of Fig. 6(b) was almost zero, which coincides with

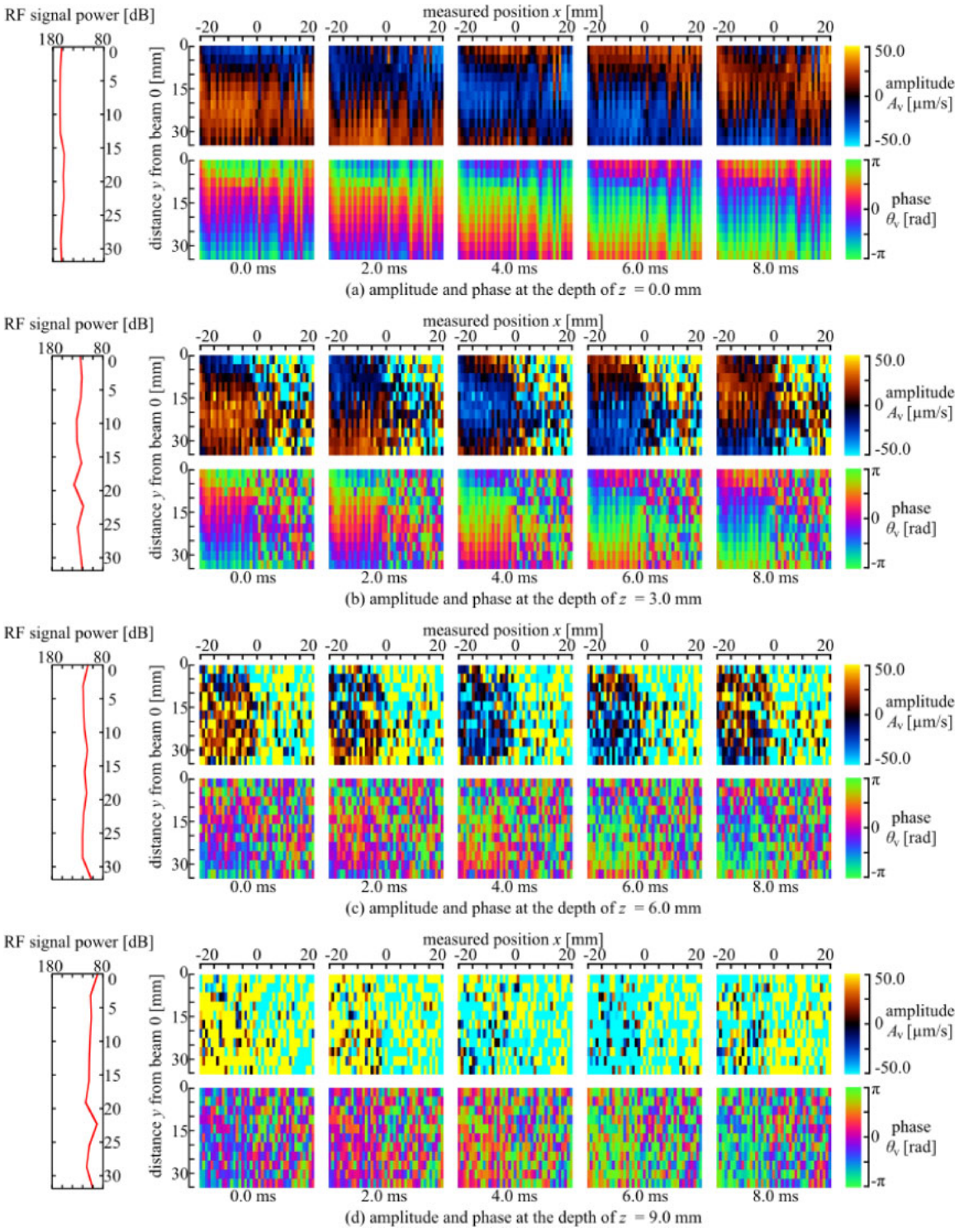

Fig. 4. (Color online) Amplitude and phase of the instantaneous velocity of the shear wave, $A_v(x, y, z, t)$ and $\theta_v(x, y, z, t)$, at the depths of (a) $z = 0$ mm, (b) $z = 3.0$ mm, (c) $z = 6.0$ mm, and (d) $z = 9.0$ mm.

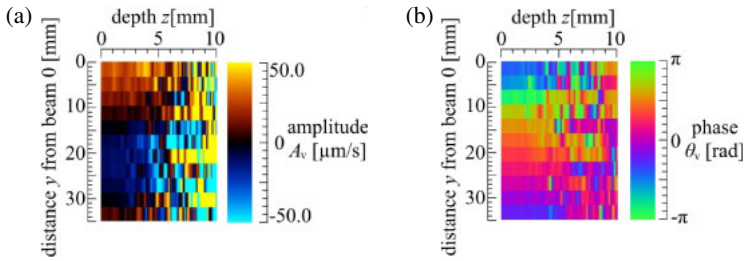

Fig. 5. (Color online) (a) Amplitude and (b) phase of the instantaneous velocity of the shear wave, $A_v(x_0, y, z, t_0)$ and $\theta_v(x_0, y, z, t_0)$, in a vertical plane of $(x_0, t_0) = (-5\,\text{mm}, 4\,\text{ms})$.

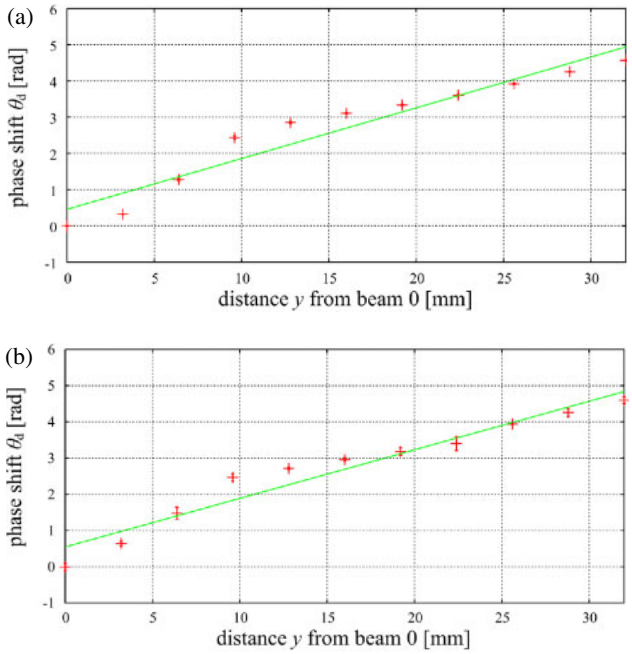

Fig. 6. (Color online) Phase shift of the instantaneous velocity at a measurement point (x_0, y, z) from the phase at a reference point (x_0, y_0, z_0) at the depths of (a) $z = 0.0$ mm and (b) $z = 3.0$ mm.

$\theta_d(x_0, y = 0, z = 0)$ at the leftmost side of Fig. 6(a), showing that the phase shift in the z-direction did not appear. This result indicates that the shear wave propagated toward the horizontal direction.

As shown in Figs. 4(a), 4(b), and 5(b), the shear wave propagated more than 30 mm along the y-axis on the x–y horizontal plane. However, as shown in Figs. 5(b), 4(c), and 4(d), it was difficult to visualize the propagation of the shear wave at the depth of $z = 5$ mm or more. This difficulty in 3D visualization would be caused by the large attenuation in the 7.5 MHz ultrasound for measurement in the phantom. Future work should include an experimental study using a phantom that satisfies the following conditions: suitability for the propagation of a 100 Hz shear wave and a low attenuation in the 7.5 MHz ultrasound for measurement.

5. Conclusions

In the present study, shear wave propagation was measured in a uniform phantom to visualize its state in a 3D space for the elastic characterization of biological soft tissue. The shear wave propagation was measured in a 3D space by scanning an ultrasound probe along the x-axis direction in the range of 41 mm. Each horizontal plane was constructed by the synchronization of signals received at various probe positions using the input signal for the acoustic radiation pressure. The proposed method succeeded in visualizing the shear wave propagation clearly in the 3D space of $35 \times 41 \times 4$ mm^3 in the x-, y-, and z-directions. The propagation velocity was estimated to be 4.5, 4.5, 4.7, and 4.7 m/s at the depths of $z = 0$, 1.0, 2.0, and 3.0 mm, respectively. These results show a high potential of the proposed method with a synchronization process in the 3D visualization of the shear wave propagation.

1) S. Shoji, *Kin Shikkan no Shindan to Chiryo* (Nagai Shoten, Osaka, 1988) p. 27 [in Japanese].
2) S. Sato and T. Inoue, *Byotai Seiri Bijuaru Mappu 4* (Igaku Shoin, Tokyo, 2010) p. 137 [in Japanese].
3) X. Qu, T. Azuma, H. Imoto, R. Raufy, H. Lin, H. Nakamura, S. Tamano, S. Takagi, S. Umemura, I. Sakuma, and Y. Matsumoto, Jpn. J. Appl. Phys. **54**, 07HF10 (2015).
4) H. Taki, K. Taki, M. Yamakawa, T. Shiina, M. Kudo, and T. Sato, Jpn. J. Appl. Phys. **54**, 07HF05 (2015).
5) Y. Nagai, H. Hasegawa, and H. Kanai, J. Appl. Phys. **53**, 07KF19 (2014).
6) H. Isono, S. Hirata, and H. Hachiya, Jpn. J. Appl. Phys. **54**, 07HF15 (2015).
7) T. M. Bui, A. Coron, J. Mamou, E. Saegusa-Beecroft, T. Yamaguchi, E. Yanagihara, J. Machi, S. L. Bridal, and E. J. Feleppa, Jpn. J. Appl. Phys. **53**, 07KF22 (2014).
8) S. Mori, S. Hirata, and H. Hachiya, Jpn. J. Appl. Phys. **53**, 07KF23 (2014).
9) H. Takahashi, H. Hasegawa, and H. Kanai, Jpn. J. Appl. Phys. **54**, 07HF09 (2015).
10) H. Taki, M. Yamakawa, T. Shiina, and T. Sato, Jpn. J. Appl. Phys. **54**, 07HF03 (2015).
11) D. Asari, H. Hasegawa, and H. Kanai, Jpn. J. Appl. Phys. **53**, 07KF21 (2014).
12) Z. Qu and Y. Ono, Jpn. J. Appl. Phys. **54**, 07HF01 (2015).
13) R. Nagaoka, R. Iwasaki, M. Arakawa, K. Kobayashi, S. Yoshizawa, S. Umemura, and Y. Saijo, Jpn. J. Appl. Phys. **54**, 07HF08 (2015).
14) R. K. Parajuli, N. Sunaguchi, R. Tei, T. Iijima, and Y. Yamakoshi, Jpn. J. Appl. Phys. **53**, 07KF30 (2014).
15) T. Shiina, Jpn. J. Appl. Phys. **53**, 07KA02 (2014).
16) Japan Society of Ultrasonics in Medicine, *Shin Cho-onpa Igaku 1 Iyo Cho-onpa no Kiso* (Igaku Shoin, Tokyo, 2000) p. 115 [in Japanese].
17) M. Fatemi, L. E. Wold, A. Alizod, and J. F. Greenleaf, IEEE Trans. Med. Imaging **21**, 1 (2002).
18) M. Fatemi and J. F. Greenleaf, Proc. Natl. Acad. Sci. U.S.A. **96**, 6603 (1999).
19) K. Nightingale, M. S. Soo, R. Nightingale, and G. Trahey, Ultrasound Med. Biol. **28**, 227 (2002).
20) G. E. Trahey, M. L. Palmeri, R. C. Bentley, and K. R. Nightingale, Ultrasound Med. Biol. **30**, 1163 (2004).
21) B. J. Fahey, K. R. Nightingale, R. C. Nelson, M. L. Palmeri, and G. E. Trahey, Ultrasound Med. Biol. **31**, 1185 (2005).
22) Japan Society of Ultrasonics in Medicine, Cho-onpa Igaku **11**, 41 (1984) [in Japanese].
23) J. Bercoff, M. Tanter, and M. Fink, IEEE Trans. Ultrason. Ferroelectr. Freq. Control **51**, 396 (2004).
24) K. Masuda, R. Nakamoto, N. Watarai, R. Koda, Y. Taguchi, T. Kozuka, Y. Miyamoto, T. Kakimoto, S. Enosawa, and T. Chiba, Jpn. J. Appl. Phys. **50**, 07HF11 (2011).
25) H. Hasegawa, M. Takahashi, Y. Nishio, and H. Kanai, Jpn. J. Appl. Phys. **45**, 4706 (2006).
26) Y. Odagiri, H. Hasegawa, and H. Kanai, Jpn. J. Appl. Phys. **47**, 4193 (2008).
27) Z. Wu, K. Hoyt, D. J. Rubens, and K. J. Parker, J. Acoust. Soc. Am. **120**, 535 (2006).
28) K. Tachi, H. Hasegawa, and H. Kanai, Jpn. J. Appl. Phys. **53**, 07KF17 (2014).
29) H. Kanai, M. Sato, Y. Koiwa, and N. Chubachi, IEEE Trans. Ultrason. Ferroelectr. Freq. Control **43**, 791 (1996).
30) H. Kanai, H. Hasegawa, N. Chubachi, Y. Koiwa, and M. Tanaka, IEEE Trans. Ultrason. Ferroelectr. Freq. Control **44**, 752 (1997).